

Supplementary Information

Methods

The isothermal remanent magnetization (IRM) in our study was imparted stepwise (~80 steps) up to a maximum peak field of 1.5 T and was measured with a vibrating sample magnetometer (VSM, Princeton Measurements Corporation, MicroMag Model 2900). The acquisition curves were decomposed into coercivity components using the fitting program of Kruiver et al. (2001), limited to symmetric distributions in the logspace.

The high resolution FORCs were measured with the MicroMag Model 2900 VSM using measurement parameters specified by Egli et al. (2010) for optimal detection of magnetofossils. The FORC diagrams were processed using the FORClab software of Winklhofer and Zimanyi (2006).

A Quantum Design SQUID magnetometer (MPMS) was used to monitor the loss of field-cooled remanence up upon warming through the Verwey transition. The field cooled remanence was obtained by cooling from 300 K to 10 K in a high magnetic field of 2.5 T.

The MPMS was also used for thermal cycling experiments (Carter-Stiglitz et al, 2006). The high coercivity fraction of the IRM (HIRM), representative of the hematite-carried remanence, was obtained by imparting a remanence in a 5T field at room temperature and then partially demagnetizing it with a maximum field of 0.18 T to eliminate the magnetite/maghemite contribution. The HIRM was then measured on cooling from 300 to 10 K, then on warming from 10 to 400 K, and cooling again from 400 to 300 K.

References

- Carter-Stiglitz, B., Banerjee, S. K., Gourlan, A., and Oches, E., 2006, A multi-proxy study of Argentina loess: Marine oxygen isotope stage 4 and 5 environmental record from pedogenic hematite: *Palaeogeography, Palaeoclimatology, Palaeoecology*, v. 2391, p. 45-62.
- Egli, R., Chen, A.P., Winklhofer, M., Kodama, K.P., and Horng, C.-S., 2010, Detection of noninteracting single domain particles using first-order reversal curve diagrams: *Geochemistry, Geophysics, Geosystems*, v. 11, Q01Z11, <http://dx.doi.org/10.1029/2009GC002916>.
- Hori, R., 1992, Radiolarian Biostratigraphy at the Triassic/Jurassic Period Boundary in Bedded Cherts from the Inuyama Area, Central Japan: *Journal of Geosciences, Osaka City University*, v. 35, p. 53-65.
- Kruiver, P. P., Dekkers, M. J., and Heslop, D., 2001, Quantification of magnetic coercivity components by the analysis of acquisition curves of isothermal remanent magnetization: *Earth and Planetary Science Letters*, v. 189, p. 269–276.

Winklhofer, M., and Zimanyi, G.T., 2006, Extracting the intrinsic switching field distribution in perpendicular media: A comparative analysis: Journal of Applied Physics, v. 99, p. 08E710, doi:10.1063/1.2176598.

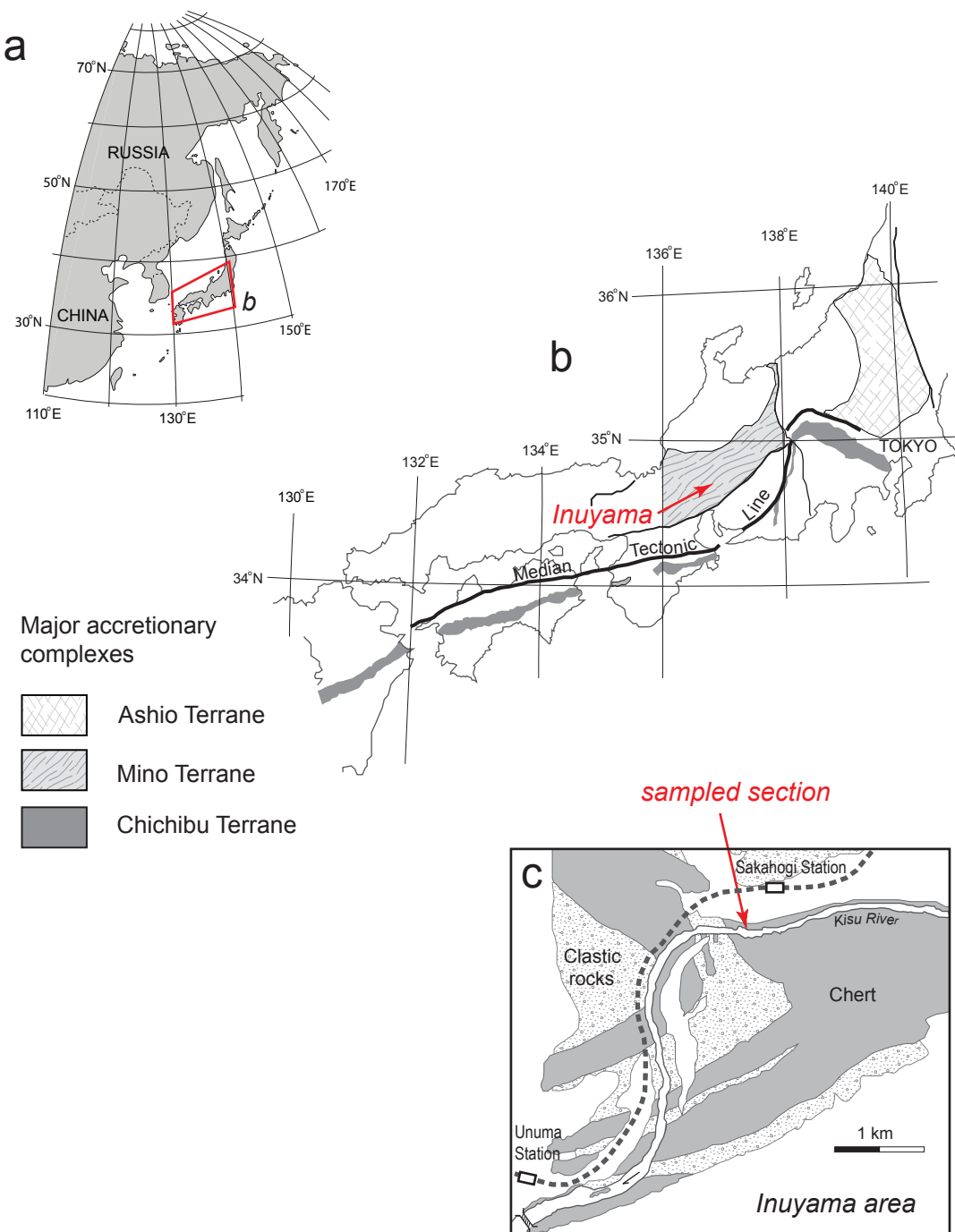


Figure DR1. Location of the studied section. Our study area is located in Central Japan (a). The Upper Triassic-Lower Jurassic (Hori, 1992) bedded chert unit is exposed as a 31 m thick, coherent thrust sheet within an accretionary pile (Mino Terrane) (b). The Triassic-Jurassic boundary section is exposed on the right bank of the Kisu River, in the vicinity of Sakahogi railway station, Gifu Prefecture (c). The GPS coordinates of the section are 35°25'23"N and 136°58'41"E.

Table DR1. IRM Component Analyses

sample	depth, cm	component 1				component 2				component 3				component 4							
		cont, %	SIRM, Am ² /kg	logB _{1/2}	B _{1/2} , mT	dp	cont, %	SIRM, Am ² /kg	logB _{1/2}	B _{1/2} , mT	dp	cont, %	SIRM, Am ² /kg	logB _{1/2}	B _{1/2} , mT	dp	cont, %	SIRM, Am ² /kg	logB _{1/2}	B _{1/2} , mT	dp
PKA-1a		0.6	6.98E-06	0.20	1.58	0.45	23.7	2.79E-04	1.25	17.78	0.39	18.3	2.15E-04	1.55	35.48	0.19	57.4	6.75E-04	2.78	602.56	0.38
PKA-1b		0.2	3.20E-06	0.20	1.58	0.45	23.1	3.10E-04	1.25	17.78	0.42	20.8	2.80E-04	1.55	35.48	0.19	55.8	7.50E-04	2.79	616.60	0.38
PKA-1c							26.7	3.62E-04	1.25	17.78	0.42	18.6	2.31E-04	1.53	33.88	0.19	54.7	6.77E-04	2.79	616.60	0.37
PKA-1-mean	76.6	0.4	5.09E-06	0.20	1.58	0.45	24.5	3.17E-04	1.25	17.78	0.41	19.3	2.42E-04	1.54	34.95	0.19	56.0	7.01E-04	2.79	611.92	0.38
Tr-18a		0.4	6.84E-06	0.30	2.00	0.45	39.8	6.84E-04	1.45	28.18	0.42	16.4	2.81E-04	1.60	39.81	0.14	43.4	7.44E-04	2.72	524.81	0.33
Tr-18b		0.3	5.00E-06	0.03	1.07	0.45	35.8	6.10E-04	1.45	28.18	0.42	13.5	2.30E-04	1.60	39.81	0.15	50.4	8.60E-04	2.71	512.86	0.34
Tr-18c		0.3	5.00E-06	0.03	1.07	0.45	36.1	6.30E-04	1.45	28.18	0.42	14.9	2.60E-04	1.60	39.81	0.15	48.7	8.50E-04	2.73	537.03	0.35
Tr-18-mean	44.2	0.3	5.61E-06	0.12	1.38	0.45	37.2	6.41E-04	1.45	28.18	0.42	14.9	2.57E-04	1.60	39.81	0.15	47.5	8.18E-04	2.72	524.90	0.34
PKA-4a		0.9	4.99E-06	0.70	5.01	0.45	19.6	1.06E-04	1.50	31.62	0.45	8.1	4.37E-05	1.58	38.02	0.15	71.1	3.87E-04	2.78	602.56	0.33
PKA-4b		0.7	4.00E-06	0.70	5.01	0.45	18.9	1.01E-04	1.55	35.48	0.45	7.6	4.06E-05	1.58	38.02	0.15	72.8	3.90E-04	2.80	630.96	0.33
PKA-4c		0.8	4.00E-06	0.70	5.01	0.45	18.4	9.50E-05	1.55	35.48	0.45	7.4	3.80E-05	1.58	38.02	0.15	73.5	3.80E-04	2.80	630.96	0.33
PKA-4-mean	33.7	0.8	4.33E-06	0.70	5.01	0.45	18.9	1.01E-04	1.53	34.20	0.45	7.7	4.08E-05	1.58	38.02	0.15	72.5	3.86E-04	2.79	621.49	0.33
PKA-5a		0.8	1.23E-05	0.40	2.51	0.45	27.2	4.11E-04	1.45	28.18	0.40	8.2	1.23E-04	1.50	31.62	0.15	63.8	9.61E-04	2.82	660.69	0.32
PKA-5b		1.3	2.00E-05	0.40	2.51	0.45	27.6	4.30E-04	1.45	28.18	0.38	5.8	9.00E-05	1.50	31.62	0.15	65.4	1.02E-03	2.81	645.65	0.33
PKA-5c		1.2	2.00E-05	0.40	2.51	0.45	30.3	5.00E-04	1.38	23.99	0.38	9.1	1.50E-04	1.45	28.18	0.15	59.4	9.80E-04	2.81	645.65	0.33
PKA-5-mean	10.9	1.1	1.74E-05	0.40	2.51	0.45	28.4	4.47E-04	1.43	26.79	0.39	7.7	1.21E-04	1.48	30.48	0.15	62.8	9.87E-04	2.81	650.67	0.33
PKA-6a		0.7	9.71E-06	0.40	2.51	0.45	31.2	4.27E-04	1.45	28.18	0.40	11.3	1.55E-04	1.55	35.48	0.15	56.7	7.77E-04	2.79	616.60	0.32
PKA-6b							38.7	5.42E-04	1.45	28.18	0.45	7.7	1.08E-04	1.58	38.02	0.17	53.6	7.50E-04	2.79	616.60	0.32
PKA-6c							34.8	4.91E-04	1.45	28.18	0.45	8.4	1.20E-04	1.58	38.02	0.17	56.8	8.00E-04	2.79	616.60	0.32
PKA-6-mean	7.3	0.7	9.71E-06	0.40	2.51	0.45	34.9	4.87E-04	1.45	28.18	0.43	9.2	1.28E-04	1.57	37.17	0.16	55.7	7.76E-04	2.79	616.60	0.32
PKA-8a		0.2	1.11E-06	0.40	2.51	0.45	9.7	6.81E-05	1.65	44.67	0.48						90.1	6.30E-04	2.95	891.25	0.28
PKA-8b		0.2	1.10E-06	0.20	1.58	0.45	8.5	5.50E-05	1.68	47.86	0.48						91.3	5.90E-04	2.96	912.01	0.27
PKA-8c		0.2	1.30E-06	0.20	1.58	0.45	9.2	6.20E-05	1.68	47.86	0.48						90.6	6.10E-04	2.94	870.96	0.28

sample	depth, cm	component 1				component 2				component 3				component 4							
		cont, %	SIRM, Am ² /kg	logB _{1/2} , mT	dp	cont, %	SIRM, Am ² /kg	logB _{1/2} , mT	dp	cont, %	SIRM, Am ² /kg	logB _{1/2} , mT	dp	cont, %	SIRM, Am ² /kg	logB _{1/2} , mT	dp				
PKA-8-mean	-2.0	0.2	1.17E-06	0.27	1.89	0.45	9.2	6.17E-05	1.67	46.80	0.48				90.7	6.10E-04	2.95	891.41	0.28		
PKA-7a		0.4	2.40E-06	0.40	2.51	0.45	7.5	4.80E-05	1.65	44.67	0.40				92.1	5.88E-04	2.81	645.65	0.38		
PKA-7b		0.6	4.00E-06	0.40	2.51	0.45	8.9	5.80E-05	1.60	39.81	0.42				90.5	5.90E-04	2.82	660.69	0.36		
PKA-7c		0.7	4.00E-06	0.40	2.51	0.45	10.2	6.20E-05	1.60	39.81	0.40				89.1	5.40E-04	2.81	645.65	0.37		
PKA-7-mean	-6.3	0.5	3.47E-06	0.40	2.51	0.45	8.9	5.60E-05	1.62	41.43	0.41				90.6	5.73E-04	2.81	650.67	0.37		
PKA-10a							2.3	1.79E-05	1.55	35.48	0.40				97.7	7.61E-04	2.76	575.44	0.35		
PKA-10b							3.2	2.50E-05	1.55	35.48	0.40				96.8	7.50E-04	2.79	616.60	0.34		
PKA-10c							3.3	2.50E-05	1.55	35.48	0.40				96.7	7.25E-04	2.79	616.60	0.35		
PKA-10-mean	-9.1						3.0	2.26E-05	1.55	35.48	0.40				97.0	7.45E-04	2.78	602.88	0.35		
PKA-9a		0.7	9.30E-06	0.40	2.51	0.40	37.3	4.65E-04	1.37	23.44	0.38				61.9	7.72E-04	2.79	616.60	0.37		
PKA-9b		2.7	3.00E-05	0.40	2.51	0.40	30.9	3.40E-04	1.40	25.12	0.45				66.4	7.30E-04	2.77	588.84	0.38		
PKA-9c		2.0	2.22E-05	0.40	2.51	0.40	29.4	3.33E-04	1.45	28.18	0.40				68.6	7.78E-04	2.78	602.56	0.39		
PKA-9-mean	-12.0	1.8	2.05E-05	0.40	2.51	0.40	32.5	3.79E-04	1.41	25.58	0.41				65.6	7.60E-04	2.78	602.67	0.38		
PKA-11a		0.1	9.67E-07	0.20	1.58	0.40	6.9	6.99E-05	1.45	28.18	0.45	5.3	5.37E-05	1.50	31.62	0.17	87.7	8.92E-04	2.81	645.65	0.35
PKA-11b		0.5	5.00E-06	0.20	1.58	0.40	7.3	8.00E-05	1.48	30.20	0.45	6.0	6.50E-05	1.50	31.62	0.17	86.2	9.40E-04	2.83	676.08	0.36
PKA-11c		0.4	4.00E-06	0.20	1.58	0.40	10.7	1.10E-04	1.40	25.12	0.45	4.4	4.50E-05	1.50	31.62	0.17	84.5	8.70E-04	2.83	676.08	0.36
PKA-11-mean	-22.0	0.3	3.32E-06	0.20	1.58	0.40	8.3	8.66E-05	1.44	27.83	0.45	5.2	5.46E-05	1.50	31.62	0.17	86.2	9.01E-04	2.82	665.94	0.36
PKA-12a		0.1	7.40E-07	0.40	2.51	0.45	18.3	1.36E-04	1.50	31.62	0.45	6.7	4.93E-05	1.50	31.62	0.15	74.9	5.55E-04	2.75	562.34	0.32
PKA-12b		0.7	5.00E-06	0.40	2.51	0.45	15.4	1.15E-04	1.45	28.18	0.45	6.0	4.50E-05	1.50	31.62	0.15	77.9	5.80E-04	2.76	575.44	0.32
PKA-12c		0.4	3.00E-06	0.40	2.51	0.45	17.0	1.30E-04	1.50	31.62	0.40	10.5	8.00E-05	1.50	31.62	0.15	72.1	5.50E-04	2.76	575.44	0.33
PKA-12-mean	-33.4	0.4	2.91E-06	0.40	2.51	0.45	16.9	1.27E-04	1.48	30.48	0.43	7.7	5.81E-05	1.50	31.62	0.15	75.0	5.62E-04	2.76	571.07	0.32
PKA-13a		1.4	1.51E-05	0.20	1.58	0.45	21.4	2.26E-04	1.50	31.62	0.45	5.7	6.03E-05	1.50	31.62	0.15	71.4	7.53E-04	2.76	575.44	0.32
PKA-13b		1.4	1.50E-05	0.20	1.58	0.45	18.6	2.05E-04	1.40	25.12	0.42	5.7	6.30E-05	1.50	31.62	0.15	74.3	8.20E-04	2.77	588.84	0.32
PKA-13c		0.5	5.00E-06	0.20	1.58	0.45	19.5	2.10E-04	1.45	28.18	0.44	6.5	7.00E-05	1.50	31.62	0.15	73.5	7.90E-04	2.77	588.84	0.32

sample	depth, cm	component 1				component 2				component 3				component 4							
		cont, %	SIRM, Am ² /kg	logB _{1/2} , mT	dp	cont, %	SIRM, Am ² /kg	logB _{1/2} , mT	dp	cont, %	SIRM, Am ² /kg	logB _{1/2} , mT	dp	cont, %	SIRM, Am ² /kg	logB _{1/2} , mT	dp				
PKA-13-mean	-53.4	1.1	1.17E-05	0.20	1.58	0.45	19.8	2.14E-04	1.45	28.31	0.44	6.0	6.44E-05	1.50	31.62	0.15	73.1	7.88E-04	2.77	584.38	0.32
PKA-14a		0.4	4.24E-06	0.40	2.51	0.35	18.3	2.02E-04	1.48	30.20	0.43	6.7	7.43E-05	1.45	28.18	0.15	74.6	8.22E-04	2.78	602.56	0.33
PKA-14b		0.5	6.00E-06	0.40	2.51	0.35	17.2	1.90E-04	1.48	30.20	0.43	5.4	6.00E-05	1.45	28.18	0.15	76.9	8.50E-04	2.78	602.56	0.34
PKA-14c		0.4	5.00E-06	0.40	2.51	0.35	16.0	1.80E-04	1.48	30.20	0.43	6.2	7.00E-05	1.45	28.18	0.15	77.3	8.70E-04	2.78	602.56	0.34
PKA-14-mean	-63.0	0.5	5.08E-06	0.40	2.51	0.35	17.2	1.91E-04	1.48	30.20	0.43	6.1	6.81E-05	1.45	28.18	0.15	76.3	8.47E-04	2.78	602.56	0.34
PKA-15a		1.0	4.46E-06	0.40	2.51	0.45	9.5	4.46E-05	1.40	25.12	0.40	9.5	4.46E-05	1.50	31.62	0.15	80.0	3.75E-04	2.73	537.03	0.35
PKA-15b		1.0	5.00E-06	0.40	2.51	0.45	8.2	4.00E-05	1.40	25.12	0.43	9.3	4.50E-05	1.50	31.62	0.17	81.4	3.95E-04	2.74	549.54	0.34
PKA-15c		0.9	4.00E-06	0.40	2.51	0.45	8.3	3.80E-05	1.40	25.12	0.42	11.1	5.10E-05	1.50	31.62	0.15	79.7	3.65E-04	2.73	537.03	0.35
PKA-15-mean	-70.6	1.0	4.49E-06	0.40	2.51	0.45	8.7	4.09E-05	1.40	25.12	0.42	10.0	4.69E-05	1.50	31.62	0.16	80.4	3.78E-04	2.73	541.20	0.35
PKA-16a		0.8	5.07E-06	0.40	2.51	0.40	4.0	2.50E-05	1.25	17.78	0.40	11.3	7.09E-05	1.55	35.48	0.18	83.9	5.27E-04	2.78	602.56	0.35
PKA-16b		0.3	2.00E-06	0.40	2.51	0.40	6.6	4.00E-05	1.40	25.12	0.45	9.1	5.50E-05	1.60	39.81	0.17	84.0	5.10E-04	2.78	602.56	0.36
PKA-16c		0.7	4.00E-06	0.40	2.51	0.40	6.5	3.50E-05	1.40	25.12	0.45	9.3	5.00E-05	1.60	39.81	0.17	83.5	4.50E-04	2.80	630.96	0.36
PKA-16-mean	-82.0	0.6	3.69E-06	0.40	2.51	0.40	5.7	3.33E-05	1.35	22.67	0.43	9.9	5.86E-05	1.58	38.37	0.17	83.8	4.96E-04	2.79	612.03	0.36
PKA-17a		0.6	4.10E-06	0.40	2.51	0.40	19.7	1.37E-04	1.40	25.12	0.45	18.7	1.30E-04	1.50	31.62	0.18	61.0	4.24E-04	2.77	588.84	0.35
PKA-17b							23.8	1.58E-04	1.42	26.30	0.45	14.3	9.50E-05	1.55	35.48	0.18	61.8	4.10E-04	2.77	588.84	0.35
PKA-17c							20.4	1.45E-04	1.42	26.30	0.45	14.9	1.06E-04	1.55	35.48	0.18	64.7	4.60E-04	2.78	602.56	0.35
PKA-17-mean	-91.3	0.6	4.10E-06	0.40	2.51	0.40	21.3	1.47E-04	1.41	25.91	0.45	16.0	1.10E-04	1.53	34.20	0.18	62.5	4.31E-04	2.77	593.42	0.35
Tr-21a		2.9	3.06E+03	0.10	1.26	0.50	14.7	1.04E-04	1.55	35.48	0.45	14.7	1.04E-04	1.60	39.81	0.17	67.6	4.78E-04	2.81	645.65	0.32
Tr-21b		0.9	6.00E-06	0.10	1.26	0.50	16.2	1.07E-04	1.55	35.48	0.45	13.4	8.90E-05	1.60	39.81	0.17	69.5	4.60E-04	2.81	645.65	0.33
Tr-21c		1.4	9.00E-06	0.10	1.26	0.50	17.2	1.08E-04	1.55	35.48	0.45	12.8	8.00E-05	1.55	35.48	0.17	68.6	4.30E-04	2.81	645.65	0.32
Tr-21-mean	-109.7	1.7	6.02E-06	0.10	1.26	0.50	16.0	1.06E-04	1.55	35.48	0.45	13.6	9.10E-05	1.58	38.37	0.17	68.6	4.56E-04	2.81	645.65	0.32

We used the algorithm of Kruiver et al. (2001) for statistical analysis of the IRM acquisition curves. The coercivity components are characterized by their magnitude (saturation magnetization SIRM), mean coercivity $B_{1/2}$ (the field at which half of the SIRM of the component is acquired), and dispersion parameter DP (equivalent to one standard deviation in log space). cont, % indicates contribution of a component into the total IRM of the sample.

The Kruiver et al. (2001) algorithm is limited to symmetric distributions in log space. However, magnetic interaction and thermal activation effects can result in departure from lognormal distributions (Egli and Lowrie, 2002, Egli, 2003, Heslop et al., 2004). To account for the skewed distributions, an additional component may be required to properly fit the data. In our samples, Component 1 likely arises from a skewed data distribution and does not represent a distinct magnetic phase. Component 2 we interpreted as detrital magnetite and/or maghemite; component 3 - as biogenic magnetite, and component 4 - as hematite.

The within-bed variations in the hematite pigment are usually small (the standard deviation values of three measurements < 10 % of the mean), testifying for the uniform diagenetic conditions during the bed's formation. The within-bed variations in the detrital and biogenic magnetite components are larger (with standard deviations values up to 25% of the corresponding mean in some beds). These variations probably reflect small changes in detrital sediment supply and the heterogeneity in spatial distribution of bacterial colonies, respectively. However, the internal differences in magnetic phases content (the SIRM values) and properties (the mean coercivity and dispersion values) are generally smaller than the differences between the beds.

References:

- Egli, R., 2003, Analysis of the field dependence of remanent magnetization curves, *J. Geophys. Res.*, 108(B2), 2081.
- Egli, R., and. Lowrie, W., 2002, Anhysteretic remanent magnetization of fine magnetic particles, *J. Geophys. Res.*, 107(B10), 2209.
- Heslop, D., McIntosh, G. and Dekkers, M.J., 2004, Using time- and temperature-dependent Preisach models to investigate the limitations of modelling isothermal remanent magnetization acquisition curves with cumulative log Gaussian functions, *Geophys. J. Int.*, 157, 55–63.
- Kruiver, P. P., Dekkers, M.J., and Heslop, D., 2001, Quantification of magnetic coercivity components by the analysis of acquisition curves of isothermal remanent magnetisation, *Earth Planet. Sci. Lett.*, 189, 269–276.